Open-Loop Responses of Droplet Vaporization to Linear Normal Acoustic Modes

S.Y. Kim, W.S. Yoon
Department of Mechanical Engineering, The Graduate School of Yonsei University
Yonsei University 134 Sinchon-dong, Seodaemun-gu, Seoul 120-749, Korea

Keywords: vaporization, droplet, response, phase equilibrium

Abstract

In order for studying pressure-coupled dynamic responses of droplet vaporization, open-loop experiment of an isolated droplet vaporization exposed to pressure perturbations in stagnant gaseous environment is numerically conducted. Governing equations are solved for flow parameters at gas and liquid phases separately and thermodynamic parameters at the interfacial boundary are matched for problem closure. For high-pressure effects, vapor-liquid interfacial thermodynamics is rigorously treated. A series of parametric calculations in terms of mean pressure level and wave frequencies are carried out employing a n-pentane droplet in stagnant gaseous nitrogen. Results show that wave instability in view of pressure-coupled vaporization response seems more susceptible at higher pressures and higher wave frequencies. Mass evaporation rate responding to pressure waves is amplified with increase in pressure due to substantial reduction in latent heat of vaporization. Augmentation of perturbation frequency also enhances amplification due to the reduction of phase differences between pressure perturbation and surface temperature fluctuation.

Introduction

Combustion instability has haunted the development of many high-performance combustors for more than forty years. This problem severely impairs engine operations and often leads to catastrophic consequences. For most liquid-fueled systems, propellants are delivered into a combustion chamber as a spray of droplets. Since droplet vaporization represents a rate-controlling process in the combustors, the dynamic behavior of spray combustion is a statistical consequence of the vaporization characteristic of an individual droplet. Thus understanding the responses of droplet vaporization to perturbing flow parameters is essential in treating combustion instability.

Since the sixties, studies on dynamic responses of droplet vaporization and combustion to flow parameter perturbation have been made and representatives are by Strahle[3], Heidmann and Wieber[4], Allison and Faeth[5], Tong and Sirignano[6-8]. In this era, a troublesome high-frequency combustion instability was a critical issue in rocket industry and most instability prediction models include the needs of certain response model in which the mass fluctuation is expressed in terms of wave parameters. The problem can be closed with a response model (or function) and prediction method of wave amplification and corresponding resonant combustion becomes complete. Strahle[3] examined droplet-vaporization responses in a forced convective field in which a small amplitude sound wave was introduced into the free stream. Heidmann and Wieber[4] studied the vaporization response of n-heptane droplets to traveling transverse oscillation in combustors over a fairly wide range of flow conditions. In their study, the peak response occurs when the droplet lifetime is approximately equal to the oscillation period. Allison and Faeth[5] studied the response function of a burning liquid monopropellant strand to imposed pressure oscillations, and found that the combustion response tends to peak in two frequency ranges. Tong and Sirignano[6-8] implemented transient heating and mass diffusion models for the liquid phase and proposed that the unsteady droplet vaporization is a potential mechanism for driving combustion instabilities. Although the preceding studies have provided significant information revealing the underlying mechanisms involved in droplet vaporization response, a number of fundamental issues related to high-pressure effects remain to be solved.

In the present study, pressure-coupled response of droplet vaporization is modeled and numerically experimented at different pressures and different frequencies. Calculation of high-pressure drop vaporization with perturbation is conducted with a flash evaporation calculation for vapor-liquid equilibrium at the drop surface. Transient, spherically symmetric drop vaporization at higher (but still subcritical) ambient pressures is formulated to simulate gas- and liquid-phase processes. Gas and liquid phase processes are formulated for a spherically symmetric droplet vaporizing in forced oscillatory environments. A unified property evaluation scheme based on the Soave-Redlich-Kwong equation of state and the extended corresponding-state principle is adopted. In order to investigate the effects of pressure perturbations on droplet vaporization, n-pentane droplets are tested as liquid phases in nitrogen gaseous environments, respectively, and discussions are made.

Open-loop responses of evaporating droplet

When a fluid is placed into motion, wave fluctuations can occur as the result of changes in pressure, velocity, and entropy. For compressible high temperature gases flowing at supersonic speed,

entropy waves are predominant. On the other hand, for incompressible fluids flowing at subsonic speed, turbulence, and/or vortex motions lead to unstable hydrodynamic waves. Acoustic waves at all flow speed regimes, both linear and nonlinear, are accompanied by pressure changes. Thus, in the present study, only the pressure-coupled vaporization responses are investigated.

Figure 1 shows the situation examined, a vaporizing droplet suddenly introduced and exposed to oscillatory pressures in a non-convective gaseous environment. This problem configuration is lacking in a typical resonating structure since perturbation is unilaterally enforced (gas-to-liquid phase only) and the processes are not interactive, and effects of perturbed thermodynamic parameters are not fed-back to alter the general profiles of gas-phase acoustics. However, this type of open-loop response model exhibits certain merits such that vaporization is isolated from a boundary-defining acoustics, is not hindered by the grid resolution problem for orderly larger gas phase space, and thus helps researchers concentrate more on revealing fundamental causes conducting this interesting phenomena. In the present analysis, vaporization of an n-pentane droplet in nitrogen gas environment.

Governing equation and numerical strategy

A theoretical-numerical framework solves the fully-coupled conservation equations of mass, momentum, total energy, and species for both the gas and liquid phases taking full account of gas-liquid interfacial dynamics. Assumptions are: spherically symmetric mass and thermal diffusions, no forced convection and gravitation effects, viscous dissipation, thermal radiation, and chemical reactions ignored, thermodynamic phase equilibrium at the drop interfacial boundary, constant ambient gas pressure, and no Soret and Dufour effects. In Eq.(1), continuity, momentum, energy and species conservation equations for gas phase are written in a vector form

$$\frac{\partial Q}{\partial t}+\frac{\partial E}{\partial r}-\frac{\partial E_v}{\partial r}-u_g\frac{\partial Q}{\partial r}=0 \qquad (1)$$

$$Q=\begin{bmatrix}\rho\\ \rho u_r\\ \rho e_t\\ \rho Y_i\end{bmatrix} E=\begin{bmatrix}\rho u_r\\ \rho u_r^2+p\\ (\rho e_t+p)u_r\\ \rho u_r Y_i\end{bmatrix} E_v=\begin{bmatrix}0\\ \tau_{rr}\\ -q_e\\ -q_{m,1}\end{bmatrix} \qquad (2)$$

Here, ρ , u_r , u_g , p , and Y_i are density, radial velocity, grid-moving velocity, pressure, and concentration of specie i , respectively. e_t is the specific total internal energy and τ_{rr} is the normal stress. Thermal and species mass diffusions are represented by Fourier's and Fick's laws, respectively. For convenience, it is assumed that ensuing surface regression is be characterized by the motion of critical surface, and this interfacial boundary is defined as the surface where the interfacial mixture is in a state of thermodynamic equilibrium. The physical properties in each phase must be linked at the surface to provide the interfacial boundary conditions (including temperature, density, and species concentration). Phase matching is accomplished by requiring the prevalence of thermodynamic phase equilibrium and continuities of mass and energy. With a view to describe a open-loop pressure waves, a hypothetical harmonic eigenvector is assumed to be a form of $p'=\bar{p}\left(1+0.05\sin\omega t\right)$. Here, 5% of pressure perturbation is due to the experimental evidences in which 5% amplitude of chamber pressure fluctuation is a statistical locus for wave instabilities. Eq.(1) is numerically stiff to solve because of disparate eigenvalues of the flow equations and poorly coupled pressure. To circumvent this problem, Eq.(1) is preconditioned and solved by a fully coupled and time-accurate numerical scheme with a dual time-stepping integration technique.

Thermodynamic model

The result of vapor-liquid phase equilibrium is required to specify the droplet surface behavior prior to the occurrence of critical conditions. The analysis usually consists of two steps. First, an appropriate equation of state as described in the section on thermodynamic and transport properties is employed to calculate fugacities of each constituent species in both gas and liquid phases. The second step lies in the determination of the phase equilibrium conditions by equating the fugacities of vapor and liquid phases of each participating species. Specific outputs from this analysis include enthalpy of vaporization, solubility of ambient gases in the liquid phase, species concentrations at the droplet surface, and conditions for criticality. The analysis can be further applied in conjunction with the property evaluation scheme to determine other important properties such as surface tension.

Modeling of drop vaporization processes hinges on an accurate description of the gas-liquid interface. Vapor-liquid phase equilibrium at any temperature and pressure are obtained by solving the phase properties coexistence between the two phases. A liquid-vapor multi component is at equilibrium if thermal, mechanical, and chemical equilibria are achieved ($T^V=T^L$, $p^V=p^L$, $\mu_i^V=\mu_i^L$). Here, superscripts V and L represent in vapor and liquid phases, respectively, and μ_i does the chemical potential species i . It is customary to express the phase equilibrium, for convenience, in terms of

fugacity. The equality of chemical potential is equivalent to $f_i^V = f_i^L$. To get a workable relation, we need to have an expression of the fugacity in terms of temperature and volume. This can be derived from basic thermodynamic relation to yield

$$R_u T \ln \varphi_i = \int_V^\infty \left[\left(\frac{\partial p}{\partial n_i} \right)_{T,V,n_j} - \frac{R_u T}{V} \right] dV - R_u T \ln Z$$

where φ_i is the fugacity coefficient of component i, defined as $f_i / x_i p$, n_i the number of moles of pure component i, V the total volume of the system, and Z, the compressibility factor of the mixture. In the present study, flash formulation and solution procedure are selectively used for vapor-liquid equilibrium at phase interface. Equations for isothermal flash calculation are easily derived by modification of the overall and component mass conservation. However, the equations are general to all simple continuous-flow equilibrium separation process in which equilibrium constant can be determined.

An essential prerequisite for any realistic treatment of high-pressure drop behavior is the establishment of a unified property evaluation scheme capable of treating thermophysical properties of the system and its constituent species over the entire fluid thermodynamic state.[1]

Pressure-coupled responses of a evaporating droplet at high pressures

The modeled system is an isolated liquid n-pentane droplet floating in oscillating high-pressure nitrogen gas.

With a view to validating the present model, static vaporization of typical hydrocarbon droplet at different pressures is examined. In Fig. 2 temporal variations of the dimensionless droplet- d^2 at different thermodynamic conditions of (a) 1 Mpa, 669 K and (b) 5 Mpa, 493 K, respectively, are depicted and compared with measurements. In Fig.2, solid lines and solid squares indicate the present analytical and experimental[12] results, respectively. Because no conservative potential force such as gravity or buoyancy effects was considered in the problem configuration, validation should be conducted with experimental data measured at microgravity conditions. Recent experimental results of Sato et al. [12] were compared. In this experiment, a n-heptane droplet of 0.65~0.8mm initial diameters was suspended in a nitrogen gas by a quartz fiber of 0.15mm thickness supporting the droplet. In Fig. 2(a) and 2(b), agreement is satisfactory in general, but starting from excellent agreement at an earlier stage of the process, analytical solutions gradually deviates from the measurements.

A series of numerical experiments of droplet vaporization subject to pressure waves are conducted. This fashion of problem configuration is more or less unrealistic but allows researchers to focus on the various mechanisms that influence the dynamic response of droplet vaporization to pressure perturbations. The present analysis treats an n-pentane droplets situated in stagnant gaseous nitrogen environments, respectively. Vaporization of an n-pentane droplets quiescent in gaseous nitrogen, was examined with an initial drop diameter 100 μm. Initial temperatures are 300 K for liquid-phase n-pentane, and 1500 K for gaseous nitrogen. The test matrix comprises three pressures of 15, 30 and 50 atm, and a number of frequencies in the range of 300 to 5000Hz.

In order to isolate some thermodynamic parameters against which the vaporization response is not sensitive, and thus simply the analysis, pressure and temperature fluctuations due to pressure perturbation were recorded, and Fig. 3 depicts evolving pressures in gas- and liquid-phases on 3(a) and 3(b), respectively. In Fig. 3, local pressures at gas- and liquid-phase illustrate almost identical waves with no distinctive differences in their amplitudes and phases. It is evident that, due to a wavelength of enforcing pressure waves orderly larger than that of droplet diameter, the pressure can be assumed to be temporally undulating but spatially invariant and a diffusion process which is essential to the description of pressure-coupled responses may be assumed to be irrelevant to pressure perturbation.

Therefore, a need to focus on another thermodynamic parameter, temperature, is freshly made. Fig.4 depicts temporal variations of temperature at the four locations. Two of them were laid on the gas-phase whereas the other two on the liquid-phase (two location in the vicinity of interfacial boundary, one inner and one outer of droplet surface, center of the droplet, and remote distance from the droplet). In accordance with pressure fluctuations, gas temperatures portrays in-phase harmonic waves at the gas phase and this type of synchronization of thermodynamic parameters is typical in gases. However, when the oscillating temperatures (heat flux) transmit the interfacial boundary and penetrate into the liquid phase, the wave is attenuated and eventually damps out when it reaches the center of the droplet. It is evident that the temperature fluctuation controlling vaporization responses occurs primarily in a region near droplet surface, and thus use of infinity conductivity model which assumes volumetric response to heat transfer, may not be allowed for the analysis of pressure-coupled response of droplet vaporization.

In order to investigate the frequency effects,

vaporization of n-pentane droplet subject to oscillating pressures is examined and the results are shown in Fig. 5 for two different frequencies of 1000 and 5000 Hz with mean ambient pressure of 15atm. Since the mechanisms associated with the vaporization process are intrinsically transient, pressure oscillation can easily couple with relevant processes and may exert significant influences on the response of vaporization rate. Here, the droplet vaporization is conditioned to be occurring at subcritical state only thus the droplet surface provides a well-defined boundary which separates the liquid from the ambient gases, and thus the vaporization rate can be easily quantified by evaluating the mass flux through the surface. Fig. 5 shows that the absolute magnitude of the vaporization response increases with frequency. At all frequencies, the time histories of mass flow rate show that the magnitude of the response increases first, mainly because of the initial heat-up in the early stage of vaporization. Generally, mass fluctuation reaches its maximum and then decays due to reduction in time for thermal diffusion with decreasing in droplet radius. With higher frequency, characteristic time of a pressure wave (a period) is much shorter than that of liquid-phase thermal inertia. The variation of the surface temperature at liquid-phase is too slow to keep in pace with the ambient pressure variation, and thus heat is more used for heating the liquid volume whereas less for supplying heat of vaporization.

Fig. 6(a) and (b) plot time histories of n-pentane mass fractions at mean pressure of 15atm and frequencies of 1000 and 5000 Hz, respectively. In Fig. 6(a), it is observed that fluctuation in gaseous mass fraction is in phase-lagged (out-of-phase) to that in liquid mass fraction. However, if the perturbation frequency is increased [Fig. 6(b)], mass fractions in liquid and gas region are oscillating with same phases (in-phase). Evidently, instability (or resonance) condition is satisfied with same phases in pressure perturbation and vaporization response, and indirectly indicates that the wave instability is more probable at high frequencies.

Fig. 7 shows time histories of surface temperature and enthalpy of vaporization for n-pentane/nitrogen system at low and high frequencies. With pressure perturbation, surface temperature fluctuation follows with a view to ensuring the thermodynamic equilibrium at interfacial boundary. This surface temperature fluctuation accompanies fluctuations of enthalpy of vaporization with no time lag and of the vaporizing mass flow rate. With higher perturbation frequency, amplitudes of AC component of surface temperature are lowered. It indicates that heat transfer mode is shifting with frequencies. With increase in frequency, heat transfer to liquid phase is conducted in a volumetric manner, and thus the amplitude of surface temperature fluctuation is decreased, whereas, at low frequency region, the heat transferred is confined in a region near the droplet surface and strong surface temperature fluctuation occurs.

Fig. 8 depicts the effects of mean pressure on droplet vaporization responses. The extent of mean pressure exerts significant influence and the fluctuation amplitude increases with increase in pressure. All the participating processes associated with static vaporization are considered to be related to this typical tendency. And one major controlling parameter would be the latent heat of vaporization. It is because that the energy required for phase transition decreases with increase in pressure and corresponding decrease in the latent heat of vaporization. As a result, higher gain amplification can be obtained at higher pressures. At lower pressure the enthalpy of vaporization is a function of temperature only, however, at high pressure, the enthalpy of vaporization is a strong function of pressure as well. When the ambient gas temperature is higher enough, increase in pressure drives the system into the critical locus and corresponding enthalpy of vaporization decreases substantially, and the vaporization becomes more sensitive to temperature fluctuation and the oscillation of vaporization mass flow rate amplifies. (Fig. 9)

It is evident that evaporation does not respond instantaneously to pressure perturbation. With increasing in frequency, phase difference between surface temperature and pressure oscillations is narrowed whereas that between pressure oscillation and fluctuation of mass flow rate does not change visibly (Fig.10). It is seen in Fig.11 that, while the frequency is fixed, phase of mass evaporation rate shifts forward close to that of pressure with augmentation in ambient pressure. This is owing to the susceptibility of heat of vaporization to high pressure. When pressure perturbation is enforced at high pressure, the amplitude of fluctuating heat of vaporization increases dramatically. It is interesting to note that the character of response is different depending on a sign of pressure perturbation. While the local pressure is increasing with positive pressure perturbation, the reduction of heat of vaporization occurs, and thus makes a shift of the peak of mass evaporation rate closer to that of pressure fluctuation and augments the vaporization rate. Whereas, when the local pressure is decreasing with negative pressure perturbation, augmentation in the heat of vaporization induces a shift of the peak of mass evaporation rate away from to that of pressure fluctuation and slows down the vaporization rate because the pressure perturbation and vaporization becomes more out-of-phase.

Concluding remarks

A numerical experiment of pressure-coupled dynamic responses of droplet vaporization was conducted employing a rigorous modeling for high-pressure drop vaporization and vapor-liquid equilibrium calculation.

The extent of mean pressure level exerts significant influence. Mass evaporation rate responding to pressure waves is amplified with increase in pressure due to substantial reduction in latent heat of vaporization. Augmentation of perturbation frequency also enhances amplification due to the reduction of phase differences between pressure perturbation and surface temperature fluctuation. At higher frequency, heat transfer to liquid phase is conducted more in a volumetric manner, whereas, at lower frequency region, the heat transferred is confined in a region near the droplet surface and strong surface temperature fluctuation occurs. While the local pressure is increasing with positive pressure perturbation, the heat of vaporization is decreased, and thus makes a shift of the peak of mass evaporation rate closer to that of pressure fluctuation and augments the vaporization rate, and vice versa. It is generally observed that wave instability in view of pressure-coupled response is more susceptible at higher mean pressure and higher frequency.

References

1) K.W.Lee, J.W.Chae, J.Y.Lee and W.S.Yoon, "Analysis of High-Pressure Drop Vaporization with Flash Vapor-Liquid Equilibrium Calculation, Int. Comm. Heat Mass Transfer, vol.30, No.5. pp.633-641,2003
2) Priem. R. J. and Guentert. D. C. , 1962 "Combustion Instability Limits Determined by a Nonlinear Theory and a One-Dimensional Model." NASA
3) Strahle.W.C.,1965, "Periodic solutions to a Convective Droplet Burning Problem" Proceedings of Tenth Symposium on Combustion. The Combustion Institute. Pittsburgh.PA. pp.1315-1325
4) Heidmann. M.F. and Wieber.P.R., "An Analysis of the Frequency Response Characteristics of Propellant Vaporization." NASA TN D-3749
5) Allison.C.B. and Faeth.G.M., 1975, "Open-Loop Response of a Burning Liquid Monopropellant." AIAA Journal. Vol. 13. October pp.1287-1294
6) Tong.A.Y. and Sirignano. W.A., 1986, "Multicomponent Droplet Vaporization in a High Temperature Gas." Combustion and Flame. Vol.66 pp.221-235
7) Tong.A.Y. and Sirignano.W.A., 1986, "Multicomponent Transient Droplet Vaporization : Integral Equation Formulation and Approximate Solution." Numerical Heat Transfer. Vol.10. pp.253-278
8) Tong.A.Y.and Sirignano.A.,1987,"Vaporization Response of Fuel Droplet in Oscillatory Field." ASME National Heat Transfer Conference. Paper No.87-HT-58
9) Takahashi, S., J.,1974, Chem. Eng.(Japan), 417
10) King,C.J.,1980, Separation Processes(2nd ed)McGraw-Hill, New York, pp.64-80
11) Rachford, H.H.Jr., Rice, J.D.,1952, Tech, 4, No.10
12) H.Nomura, Y.Ujiie,H.J.Rath, J.Sato, M.Kono, Proc.Combust.Inst.26(1996)1267

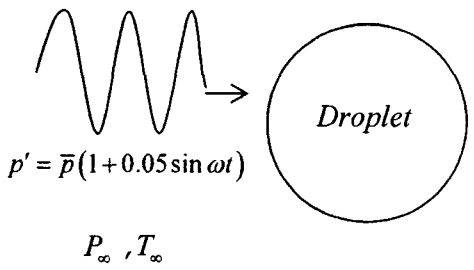

Fig.1 Schematic of pressure-coupled responses of a droplet stagnant in high-pressure environment

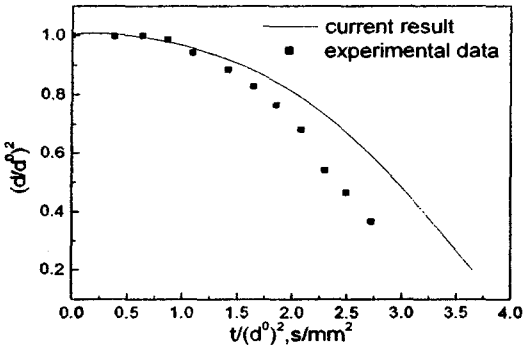

(a) $P_a = 1MPa,\ T_a = 669K$

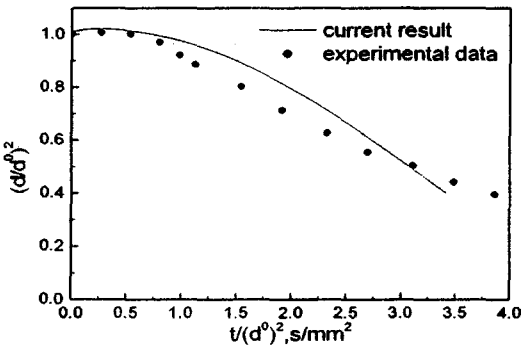

(b) $P_a = 5MPa,\ T_a = 493K$

Fig.2 Temporal evolutions of dimensionless d^2 of n-heptane/nitrogen system [12]

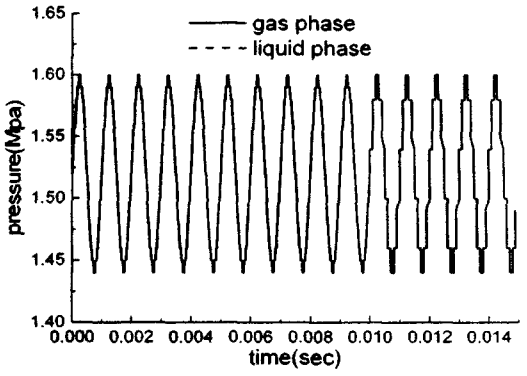

Fig.3 Temporal evolution of pressures in gas- and liquid phases (n-Pentane/Nitrogen system, 15atm 1000Hz)

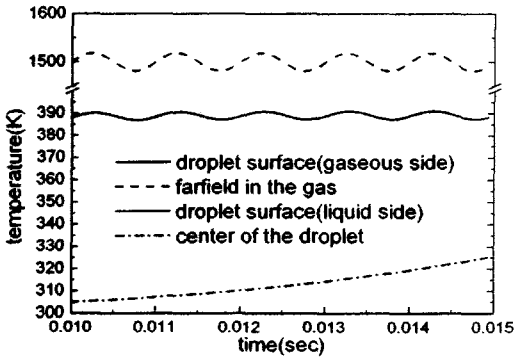

Fig.4 Temporal variations of temperatures subject to pressure perturbation(n-Pentane/Nitrogen System, $15atm$ $1000Hz$)

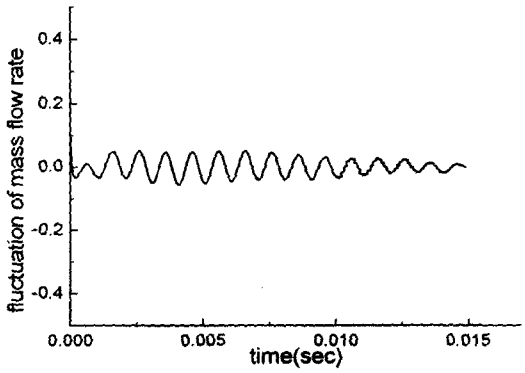

(a) $15atm\ 1000Hz$

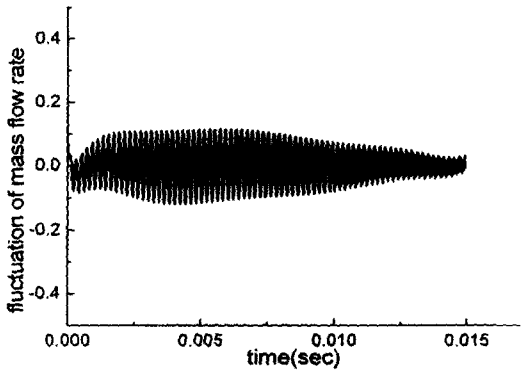

(b) $15atm\ 5000Hz$

Fig.5 Effects of frequency of pressure perturbation on vaporization rate (n-Pentane/Nitrogen System)

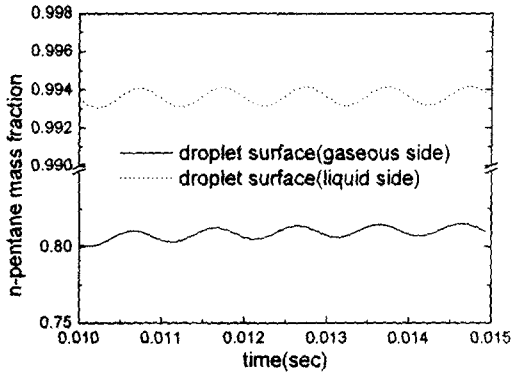

(a) $f = 1000Hz$

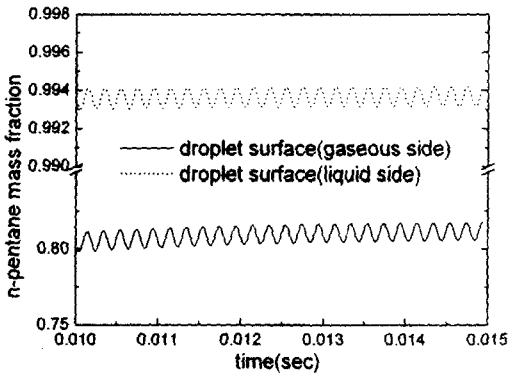

(b) $f = 5000Hz$

Fig. 6 Fluctuation of n-Pentane mass fraction in a vicinity of droplet surface n-Pentane/Nitrogen System(15atm)

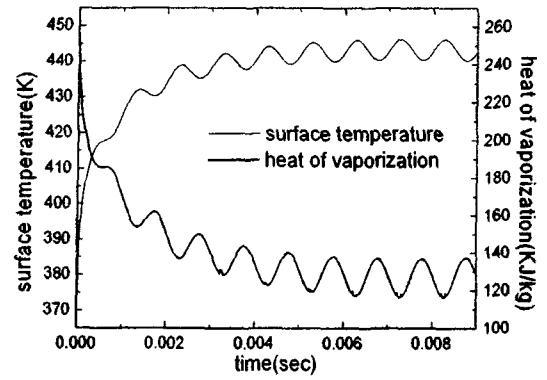

(a) $f = 1000Hz$

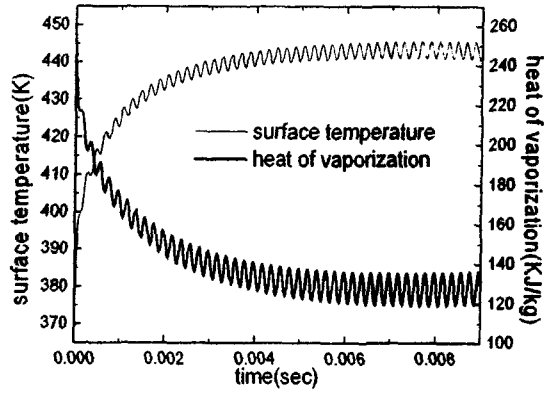

(b) $f = 5000Hz$

Fig. 7 Fluctuation of surface temperature and heat of vaporization in a vicinity of droplet surface, n-Pentane/Nitrogen System (50atm)

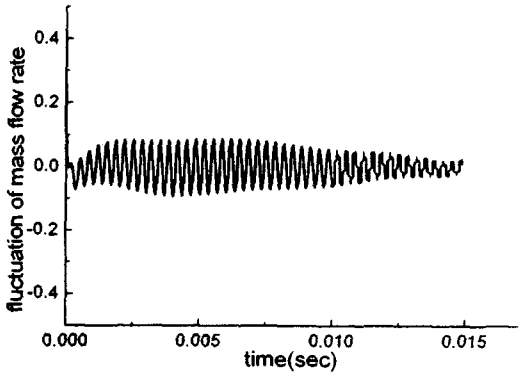

(a) $P_a = 15atm$

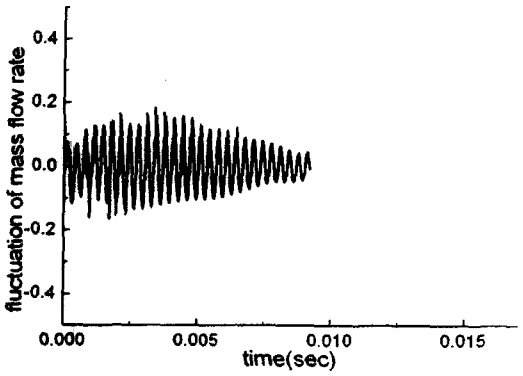

(b) $P_a = 50atm$

Fig. 8 Effects of mean-pressure magnitude on vaporization rate (n-Pentane/Nitrogen System, $f = 3000Hz$)

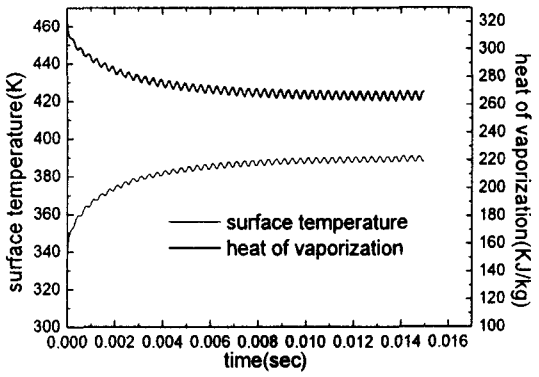

(a) $P_a = 15atm$

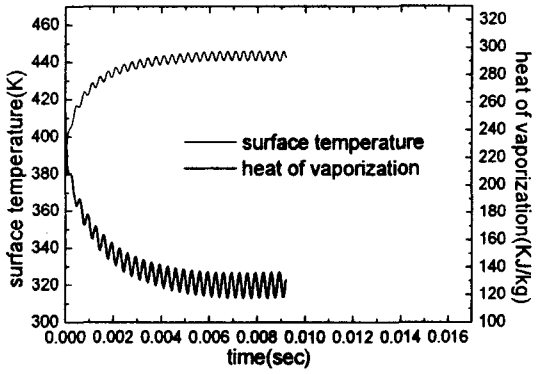

(b) $P_a = 50atm$

Fig. 9 Fluctuation of surface temperature and heat of vaporization in a vicinity of droplet surface, n-Pentane/Nitrogen System ($f = 3000Hz$)

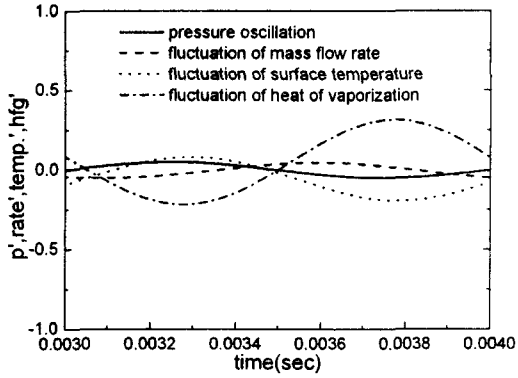

(a) $f = 1000Hz$

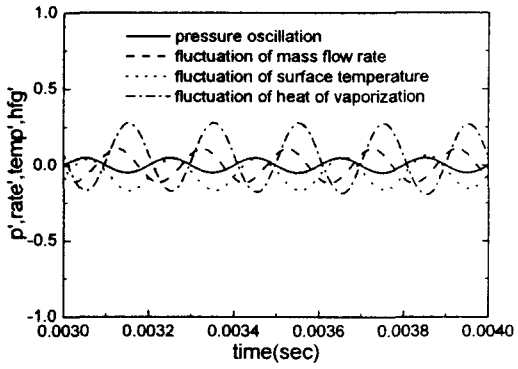

(b) $f = 5000Hz$

Fig. 10 Fluctuating flow parameters at different frequencies n-Pentane/Nitrogen System ($15atm$)

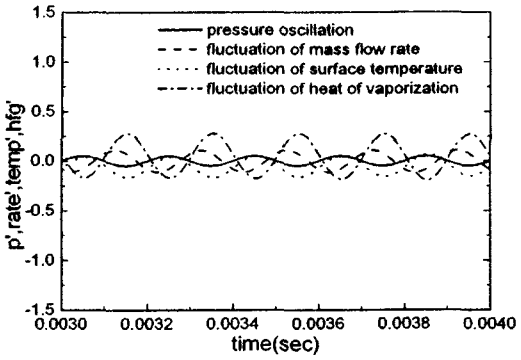

(a) $P_a = 15atm$

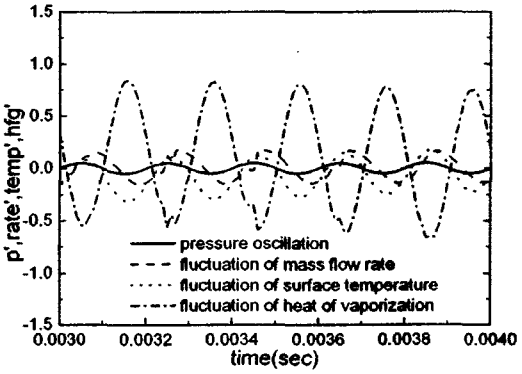

(b) $P_a = 50atm$

Fig. 11 Fluctuating flow parameters at different pressures. n-Pentane/Nitrogen System ($f = 5000Hz$)